NEOPLASIA
www.neoplasia.com

Volume 13 Number 8 August 2011 pp. 704–715 704

Identification of Oncogenic Point Mutations and Hyperphosphorylation of Anaplastic Lymphoma Kinase in Lung Cancer[1,2]

Yi-Wei Wang*,†, Pang-Hsien Tu*,†, Kuen-Tyng Lin†, Shu-Chen Lin†, Jenq-Yuh Ko‡ and Yuh-Shan Jou*,†

*Graduate Institute of Life Sciences, National Defense Medical Center, Taipei, Taiwan; †Institute of Biomedical Sciences, Academia Sinica, Taipei, Taiwan; ‡Departments of Otolaryngology, National Taiwan University Hospital and College of Medicine, National Taiwan University, Taipei, Taiwan

Abstract

The oncogenic property of anaplastic lymphoma kinase (ALK) plays an essential role in the pathogenesis of various cancers and serves as an important therapeutic target. In this study, we identified frequent intragenic loss of heterozygosity and six novel driver mutations within *ALK* in lung adenocarcinomas. Overexpression of H694R or E1384K mutant ALK leads to hyperphosphorylation of ALK, and activation of its downstream mediators STAT3, AKT, and ERK resulted in enhanced cell proliferation, colony formation, cell migration, and tumor growth in xenograft models. Furthermore, the activated phospho-Y1604 ALK was increasingly detected in 13 human lung cancer cell lines and 263 lung cancer specimens regardless of tumor stages and types. Treatment of two different ALK inhibitors, WHI-P154 and NVP-TAE684, resulted in the down-regulation of aberrant ALK signaling, shrinkage of tumor, and suppression of metastasis and significantly improved survival of ALK mutant-bearing mice. Together, we identified that novel ALK point mutations possessed tumorigenic effects mainly through hyperphosphorylation of Y1604 and activation of downstream oncogenic signaling. The upregulated phospho-Y1604 ALK could serve as a diagnostic biomarker for lung cancer. Furthermore, targeting oncogenic mutant ALKs with inhibitors could be a promising strategy to improve the therapeutic efficacy of fatal lung cancers.

Neoplasia (2011) 13, 704–715

Introduction

Lung cancer is the leading cause of cancer mortality worldwide, which claims approximately 1.3 million deaths annually. Lung cancers are broadly classified into non–small cell lung cancers (NSCLCs) and small cell lung cancers (SCLCs), which account for approximately 80% and 20% of total cases, respectively [1]. Among NSCLCs, the adenocarcinoma constitutes more than 40% of lung cancer patients and is increasing in recent decades. It has replaced squamous cell carcinoma to become the leading subtype of lung cancer [2]. Recent advances in genetic studies of lung adenocarcinoma revealed somatic alterations in genes including *p53*, *KRAS*, *EGFR*, *HER2*, *c-MET*, *LKB1*, *PIK3CA*, and *BRAF* that conferred selective advantages of cancer cells in growth, apoptotic resistance, angiogenesis, and metastasis [3–13]. *EGFR* mutations were commonly observed in nonsmoking adenocarcinomas of Asian female patients (<40%) but were less frequent in those of non-Asian patients. In contrast, *KRAS* and *LKB1* mutations were frequently detected in non-Asian and smoking patients (<30% and <34%, respectively) but were less frequently found in Asian patients [14–17]. The status of *EGFR* is an important predicative factor of successful responses to small-molecule EGFR tyrosine kinase inhibitors, gefitinib and erlotinib [5,6]. However, the prognostic impact of

Abbreviations: ALK, anaplastic lymphoma kinase; NSCLC, non–small cell lung cancer; NPM-ALK, nucleophosmin-anaplastic lymphoma kinase; ALCL, anaplastic large cell lymphoma; EML4-ALK, echinoderm microtubule-associated protein-like 4–anaplastic lymphoma kinase; TAE684, NVP-TAE684; IP, immunoprecipitation; IHC, immunohistochemistry; AIG, anchorage-independent growth

Address all correspondence to: Yuh-Shan Jou, PhD, 128, Sec 2 Yen-Chiu-Yuan Rd, Institute of Biomedical Sciences, Academia Sinica, Taipei, 11529 Taiwan.
E-mail: jou@ibms.sinica.edu.tw

[1]This work was funded by the National Research Program for Genomic Medicine of National Science Council, Taiwan (grants 91-3112-P-400-004-Y and NSC98-3112-B-001-004). The authors disclose no conflicts.
[2]This article refers to supplementary materials, which are designated by Tables W1 to W4 and Figures W1 to W7 and are available online at www.neoplasia.com.
Received 27 January 2011; Revised 16 May 2011; Accepted 18 May 2011

DOI 10.1593/neo.11222

EGFR-based target therapy on lung adenocarcinoma is controversial. Despite recent therapeutic advances, the overall 5-year survival rate for lung adenocarcinoma remains approximately 15% [18]. Therefore, discovery of novel targets for development of therapeutic strategies is in urgent need.

Anaplastic lymphoma kinase (*ALK*) was initially identified in a chromosomal translocation t(2;5)(p23;q35) associated with approximately 75% of patients with anaplastic large cell lymphoma (ALCL) [19,20]. That translocation fused the 5′ end of the *nucleophosmin* (*NPM*) to the 3′ *ALK* and resulted in the formation of a constitutively active oncogene encoding a chimeric tyrosine kinase NPM-ALK, which, in turn, led to enhanced cell proliferation, cell migration, resistance to apoptosis, and cytoskeleton reorganization. The tumorigenic property of NPM-ALK is mediated through activation of multiple interconnecting signaling pathways including Ras/ERK, JAK3/STAT3, and PI3K/AKT pathways [21]. Recently, another oncogene with the 5′ end of the *echinoderm microtubule-associated protein-like 4* (*EML4*) fused to 3′ *ALK* was identified in lung adenocarcinomas with a prevalence of ~7% of total lung cancers [22]. *EML4-ALK* also encodes a ligand-independent and constitutively active tyrosine kinase with oncogenic activity [23]. Treatments with ALK inhibitors resulted in shrinkage of lung tumors in *EML4-ALK* transgenic and xenografted models, which supported *EML4-ALK* to be a novel driver mutation and therapeutic target in NSCLCs [24,25]. Recent efforts of sequencing 623 genes involved in tumorigenesis of lung adenocarcinoma from 188 white patients identified four additional *ALK* point mutations on different protein domains (P496L, P542R, S631I, and V1135E), deposited in the database of Catalogue of Somatic Mutations in Cancer [26]. Similar to other cancers with somatic alterations in tyrosine kinases, two ALK secondary mutations, C1156Y and L1196M, were identified within the kinase domain of EML4-ALK in a patient with NSCLC who became resistant to ALK inhibitor crizotinib after successful treatment for 5 months [27]. Furthermore, *ALK* alterations were observed in other tumors such as inflammatory myofibroblastic tumors caused by *TPM4-ALK* oncogene, diffuse large B-cell lymphoma caused by *CLTC-ALK* oncogene, and sporadic and familial neuroblastomas caused by *ALK* point mutations [28–32].

Because *ALK* was located within the frequent loss of heterozygosity (LOH) region in our previous report [33] and its alterations in lung cancers remained to be determined, we therefore screened ALK point mutations and examined their pathogenic roles in lung adenocarcinomas.

Materials and Methods

Patients with Lung Adenocarcinoma

Forty-eight pairs of lung adenocarcinoma and their tumor-adjacent nonneoplastic tissues were obtained from patients who underwent surgical resection at the National Taiwan University Hospital from June 2000 to December 2002, after approval from the research ethics committee of the hospital. All clinical data of patients were recorded, including sex, age, smoking status, location of the tumor, and ensuing distinct metastases after surgery. There were 29 men and 19 women, with a mean age of 64 years, ranging from 38 to 79 years. All women were nonsmokers and 15 men had smoking history. Clinicopathologic features of 48 patients are listed in Table W1. All specimens either OCT-embedded frozen or formalin-fixed tissues were sectioned and stained with hematoxylin and eosin for microscopic examination. Histologic diagnosis and pathologic features were obtained according to the International Staging System for Lung Cancer, including tumor cell type, direct invasion to surrounding structures, and regional lymph node metastasis.

DNA Extraction from Microdissected Lung Adenocarcinomas and Mutation Detection

Lung adenocarcinoma sections (4 μm) either OCT-embedded frozen tissues or deparaffinized formaldehyde-fixed, paraffin-embedded tissues were stained with hematoxylin and eosin for pathologic distinction of tumor and nonneoplastic cells as per the pathologist on each sample. Microdissection experiments were performed using either the PixCell II laser capture microdissection apparatus (Arcturus Biosciences, Mountain View, CA) or the Laser Microdissection System (Leica LMD, Wetzlar, Germany) according to manufacturer's instructions. Greater than 70% purity of cancerous and tumor-adjacent normal cells on 8 to 10 tissue sections (100-300 cells per section) were isolated and pooled separately to yield approximately 2000 to 4000 cells per sample. An estimated 1000 microdissected cells were digested in 50 μl of lysis buffer (10 mM Tris-HCl, pH 8.0, 1% Tween-20) and incubated with 6% Chelex 100 (Sigma, St Louis, MO) and 0.1 mg/ml proteinase K for 24 hours at 56°C. The protease-treated DNA mixture was heat inactivated after incubating for 10 minutes at 95°C and made ready for polymerase chain reaction (PCR). The exon and intron boundaries of *ALK* were based on annotations in the Ensembl database (http://www.ensembl.org), and their primers were designed by the Primer3 Web site (http://frodo.wi.mit.edu/primer3/) (Table W2). LCM-purified samples were amplified in a 10-μl volume contained 0.05 μM primers, 250 μM of each dNTPs, 2.5 mM $MgCl_2$, and 0.5 U of FastTaq DNA polymerase (Roche Applied Science, Mannheim, Germany) at 95°C for 10 minutes and cycled at 94°C for 10 seconds and at 55°C for 10 seconds and at 72°C for 20 seconds for 45 to 60 cycles. PCR products were purified by ExoSAP-IT PCR Clean-up Kit (GE Healthcare, Buckinghamshire, United Kingdom) in 96-well format and sequenced by ABI 3730 DNA sequencing analyzer (Life Technologies, Carlsbad, CA). Mutation detection was conducted by using Sequencher 4.1.4 (Gene Codes, Ann Arbor, MI). Mutated exons were confirmed again by reversed primer. Mutation data also validated by two additional researchers and by using Mutation Survivor software (version 3.0; SoftGenetics, State College, PA).

Cell Lines

Thirteen human lung cancer cell lines (A549, CL1-0, CL1-3, CL1-5, H23, H226BR, H358, H460, H661, H928, H1299, H1435, and H1437) were included in this study. Two near-normal bronchial epithelial cells (BEAS-2B and NL20) were kindly provided by Dr Cheng-Wen Wu from our institute and by Dr Wayne Chang from the National Institute of Cancer Research of the National Health Research Institutes at Miaoli, Taiwan, respectively. K562 (chronic myeloid leukemia cell line; NPM-ALK$^-$), SU-DHL (ALCL cell line; NPM-ALK$^+$), and three neuroblastoma cell lines (IMR32 [wild-type ALK], SH-SY-5Y [F1174K mutant ALK], and SK-N-SH [F1174K mutant ALK]) served as antibody controls for phospho-Y1604 ALK and ALK [30–32,34,35]. NIH3T3 cells were used to further confirm the oncogenic property of ALK mutations. All cell culture conditions and culture media were according to the ATCC (Manassas, VA) standard protocols.

Antibodies and Reagents

For Western blot analysis, membranes were probed with indicated antibodies against HA (MMS-101R; Covance, Princeton, NJ), phospho-tyrosine (4G10, 16-101; Upstate Biotechnology, Lake Placid, NY), STAT3 (sc-482; Santa Cruz, Santa Cruz, CA), and α-tubulin (MS-581; Thermo, Rockford, IL). Phospho-ALK (Tyr1604, no. 3341), phospho-AKT (Ser473, no. 9271), phospho-STAT3 (Tyr705, no. 9145),

phospho-ERK (Thr202/Tyr204, no. 9101), AKT (no. 9272), and ERK (no. 4695) antibodies were purchased from Cell Signaling (Danvers, MA). ALK antibody–conjugated beads (C26G7, no. 5611) for immunoprecipitation (IP) assay were also from Cell Signaling. For immunohistochemistry (IHC) staining assay, tissue sections were stained with the indicated antibodies against phospho-ALK (pY1604, no. 1891-1; Epitomics, Burlingame, CA), ALK (no. 4204-1; Epitomics), phospho-STAT3 (Tyr705, no. 9145; Cell Signaling), and phospho-AKT (Ser473, no. 3787; Cell Signaling). ALK inhibitors WHI-P154 (no. 420104) and NVP-TAE684 (S1108) were purchased from Calbiochem (La Jolla, CA) and Selleck (Houston, TX), respectively.

ALK Constructs and Cell Transfection

Wild-type ALK construct was subcloned by moving the full-length ALK cDNA purchased from ATCC (ATCC no. 69497; pRMS17-2) into the pcDNA3.0 vector. Six ALK mutation constructs (S413N, V597A, H694R, G881D, Y1239H, and E1384K) were generated from the pcDNA3.0–wild-type ALK construct by site-directed mutagenesis using QuickChange Kit (Stratagene, La Jolla, CA). The sequences of wild-type and mutant ALK constructs were confirmed by DNA sequencing. H1299 and NIH3T3 cells were individually transfected with ALK constructs by Lipofectamine 2000 (Invitrogen, Carlsbad, CA) and independently selected for transfectants derived from mixed G418 (800 μg/ml) resistant clones.

Western Blot and IP Analysis

Cells were lysed in RIPA buffer (20 mM Tris, 150 mM NaCl, 1 mM EDTA, 1% NP-40, 1 mM phenylmethylsulfonyl fluoride, and 1 mM dithiothreitol) with addition of protease inhibitor cocktail (1697498; Roche). For phosphorylated protein detection, additional phosphatase inhibitor cocktail (no. 524625; Calbiochem) was added into RIPA/protease inhibitor mixture. Protein concentration was measured by BCA protein assay kit (Pierce Chemical, Rockford, IL). Equal amounts of cell lysates were subjected to SDS-PAGE, transferred to NC membranes, and probed with the indicated antibody for protein detection. For IP assay, equal amounts of cell lysate were first incubated with the anti-HA antibody for 1 hour and, subsequently, reacted with protein A/G–conjugated beads overnight at 4°C or directly incubated with the anti-ALK antibody–conjugated beads. The pulled-down beads were washed and subjected to Western blot analysis for protein detection.

Immunohistochemistry

IHC assays were performed on six human lung cancer tissue sections with ALK mutations, four human lung cancer sections without ALK mutations, two normal human lung sections (LUN01 and LUN02) from Pantomics (Richmond, CA), five human lung cancer tissue arrays containing 37 normal lung sections and 263 lung cancer sections from Pantomics (LUC961, LUC962, LUC1501, LUC1502, and LUC1503), three human tissue arrays from US Biomax (Rockville, MD) including ALCL (NHL803b), rhabdomyosarcoma (SO751), and normal lymph node (NHL801), and OCT-embedded frozen tumor sections prepared from the xenografted nude mice. After deparaffinization, all sections were treated with 3% H_2O_2 buffer for 30 minutes to inactivate the endogenous peroxidase activities and then incubated in 0.01 M sodium citrate buffer for antigen retrieval. After blocking with 10% normal goat serum, these sections were reacted with indicated antibodies at 4°C for overnight. Subsequently, these sections were incubated with HRP polymer conjugate (no. 87-9663; Invitrogen), diaminobenzidine staining, and then Mayer hematoxylin (S3309; DAKO, Glostrup, Denmark).

Cell Proliferation Assay

A total of 1×10^3 cells in each well were seeded in 96-well plate. After the indicated culture time, 10 μl of WST-1 reagent (11644807001; Roche) was added into each well for incubation at 37°C for 40 minutes, and the absorbance was then measured at 450 nm.

Boyden Chamber Assay

Cell migration capability was examined by Boyden chamber assay. A total of 2×10^4 cells were seeded into the cell migration insert (353097; Falcon, Franklin Lakes, NJ) containing 350 μl of Dulbecco modified Eagle medium and then placed into the well containing 750 μl of 10% fetal bovine serum/Dulbecco modified Eagle medium in a 24-well plate (353504; Falcon). After 18 hours of incubation, migrated cells were fixed with 100% methanol and stained with Giemsa solution (Merck, Whitehouse Station, NJ). The number of migrated cells was counted by the Image-Pro Plus analysis program (MediaCybernetic, Bethesda, MD).

Anchorage-Independent Growth Assay

A total of 2×10^4 cells were first mixed with a final 0.3% agarose solution and plated into the 60-mm plate dish coated with 0.5% agarose solution. After 28 days of incubation, these plates were dehydrated at room temperature and then stained with 0.3% crystal violet solution for colony visualization. The number of colonies formed was counted by the Image-Pro Plus analysis program.

In Vitro *Kinase Assay*

In vitro ALK activity of H1299 transfectants was measured by universal tyrosine kinase assay kit (MK410; Takara, Shiga, Japan). In brief, cells were first lysed in lysis buffer. After quantifying the protein concentration using the BCA assay, equal amounts of cell lysates were immunoprecipitated using the anti-HA antibody, and the ALK-precipitated complex was then added into the wells coated with poly-Glu-Tyr substrate. After 30 minutes of incubation, the peroxidase-conjugated anti-phosphotyrosine antibody was added into the wells. After incubating with the Horseradish peroxidase (HRP) substrate solution, the wells were read in an ELISA reader set at an absorbance of 450 nm.

Immunofluorescence

After the cells were fixed in 4% formaldehyde/phosphate-buffered saline and permeabilized in 0.5% Triton X-100/phosphate-buffered saline, the ALK protein was stained with the anti-HA primary antibody and secondary antibody conjugated with tetramethylrhodamine-5-isothiocyanate and was visualized under a confocal laser scanning microscope. The nuclei were counterstained with 4′-6-diamidino-2-phenylindole (DAPI).

Short Hairpin RNA–Lentivirus Infection

ALK short hairpin RNA (shRNA) constructed in pLKO.1 lentiviral vector was obtained from the National RNAi Core Facility of Taiwan, with a targeted sequence of CTGGTCATAGCTCCTTGGAAT. For lentivirus production, 293T cells were cotransfected with *ALK* shRNA in pLKO.1 lentiviral vector, packaging plasmids pMD.G and pCMVΔR8.91. After 4 days of transfection, virus-containing media were collected and filtered. H1299 cells that stably expressed wild-type and mutant ALKs were infected with virus-containing media in the presence of polybrene.

In Vivo *Xenograft Tumor Formation Assay*

The animal protocol was approved by the Institutional Animal Safety Committee of Academia Sinica. A total of 1×10^6 H1299 cells that stably expressed wild-type or mutated ALKs were mixed with Matrigel (356237; BD, Franklin Lakes, NJ) and then subcutaneously injected into the right flank of 4-week-old BALB/c *NU* mice. Tumor volumes were measured weekly and calculated according to the formula: volume = length × width^2 × 0.52. When the mean tumor volume reached 20 to 50 mm^3, nude mice were randomly divided into two groups and treated with the ALK inhibitor WHI-P154 or NVP-TAE684 daily. WHI-P154 was dissolved in dimethyl sulfoxide (DMSO) and intravenously injected at 1 mg/kg per day. NVP-TAE684 was resuspended in 10% 1-methyl-2-pyrrolidinone/90% PEG 300 (Sigma, St Louis, MO) solution administered daily by oral gavage at 10-mg/kg concentration as described previously [36].

In Vivo *Metastasis Assay*

For *in vivo* metastatic assay, H1299 cells that stably expressed wild-type or mutant ALKs were infected by GFP-lentivirus to generate the GFP fluorescence-labeled cells. A total of 2×10^6 cells were injected into nude mice through tail vein. To investigate the effect of WHI-P154 on lung metastasis, nude mice were intravenously injected with WHI-P154 (1 mg/kg per day) daily 14 days after injecting GFP-labeled H1299 stable cells. Survival rate was recorded daily, and the injected mice were killed after 105 days. Lung metastases of GFP-labeled H1299 stable cells were visualized using a fluorescence stereomicroscope.

Statistical Analysis

Data are presented as mean ± SD. For the comparison of different groups, Student's *t* tests were used to determine the statistical significance. For IHC correlation between the expression of phospho-Y1604 ALK and the total ALK, the Pearson correlation coefficient was calculated in SAS (SAS Institute, Inc, Cary, NC). For survival analysis, a multiple-comparison adjustment to the *P* values for the paired comparison between wild type with each group was also calculated in SAS.

Results

Identification of Tumorigenic Somatic ALK Mutations

Because *ALK* is located within the 2p23 chromosomal region that was previously found to have LOH at a frequency of 69.4% (25/36) using the microsatellite marker *AFM198wc5* and have chromosomal amplification using comparative genome hybridization analysis [33,37,38], we hypothesized that *ALK* underwent unequal allelic amplification and resulted in frequent LOH. Therefore, *ALK* gene was selected for further mutational analyses. Consistent with our expectation, six novel *ALK* mutations different from the four mutations reported in the Catalogue of Somatic Mutations in Cancer database were discovered in 48 lung adenocarcinomas, but no *ALK* mutation was found in 13 lung cancer cell lines. The *ALK* mutations were confirmed by forward and reverse sequencing (Figure W1). The seven K-*ras* mutations including two hot spot mutations at codons 12 and 13 were served as system control. These six novel mutations were distributed in different protein domains, including S413N in the MAM1 domain, V597A in the MAM2, H694R in area without a defined domain, G881D in the glycine-rich domain, and Y1239H and E1384K in the kinase domain. Although all six mutations occurred in T2 stage patients, the small sample size precluded us from drawing a conclusive link between these mutations and clinical stages.

To determine whether these mutations were gain-of-function driver mutations, we individually introduced these six *ALK* mutations into the lung cancer cell line H1299, which expressed ALK protein at a level lower than other lung cancer cell lines (Figure 2*A*) and was commonly used for lung cancer studies [39,40]. As shown in Figure 1*A*, overexpression of wild-type ALK slightly increased phospho-Y1604 ALK (p-ALK; Figure 1*A*) and overall phosphorylated tyrosine signals of ALK around 250 kd (4G10; Figure 1*A*) compared with the mock control. Overexpression of V597A, H694R, G881D, or E1384K significantly enhanced the levels of phospho-Y1604 and the overall phosphorylated tyrosine signal of ALK, but the effect of S413N or Y1239H seemed negligible compared with that of wild-type ALK. These data suggested that the first four ALK mutations conferred a higher kinase activity.

To investigate the effect of individual mutant ALKs on the downstream signaling pathways, we examined the phosphorylation status of three known ALK effectors, namely, STAT3, AKT, and ERK. Again, overexpression of wild-type ALK slightly increased phospho-STAT3, phospho-AKT, and phospho-ERK compared with mock control. As expected, the V597A, H694R, G881D, and E1384K four mutants each revealed significantly enhanced downstream signaling but the S413N or Y1239H mutant did not. These results were in good agreement with the kinase activities of these mutants. Notably, among the four activating mutants, differences in the capability to activate each downstream signaling pathway were also observed. Specifically, the H694R or E1384K mutant led to further increases in the phosphorylation status of all three (STAT3, AKT, and ERK) signaling molecules compared with the wild-type counterpart. However, the V597A mutant mainly induced a higher level of phospho-ERK, but not of phospho-AKT or phospho-STAT3, and the G881D mutant significantly increased phospho-AKT and phospho-ERK expression, but left the expression of phospho-STAT3 comparable to that by wild-type ALK.

Next, we correlated the expression of phosphorylated ALK of lung adenocarcinomas with their mutational status by polymer-amplified IHC analyses using tissue sections of six ALK mutation-bearing patients, four tumors without ALK mutations from this group of 48 NSCLC patients and 2 nonneoplastic controls (Figure 1*B*). As shown, tumors carrying V597A, H694R, G881D, and E1384K mutations (*left column*) showed a higher phospho-Y1604 ALK staining intensity than two normal lungs (nos. 1 and 2; *right column*) and four adenocarcinomas (case nos. 1, 17, 19, and 30; *right column*) without ALK mutation. However, all tumors had higher phospho-Y1604 ALK intensity than normal lung sections did. These results were consistent with those obtained from the studies in H1299 cells,

To further determine the tumorigenic effects of these ALK mutations, we conducted *in vivo* tumor formation assay in nude mice. In comparison with the tumors of mock control, wild-type ALK slightly increased tumor weight 5 weeks after injection of H1299 stable cells. Tumors stably expressing each of the six ALK mutant proteins were significantly larger than those expressing wild-type ALK or control (Figure 1*C*). Altogether, these results indicated that all of these six ALK mutations were in fact gain-of-function driver mutations *in vivo*. Among them, H694R and E1384K mutants increased constitutive phosphorylation of *Y1604* ALK and its downstream STAT3, AKT, and ERK signaling efforts and exhibited the highest ability to promote tumor growth compared with the other four ALK mutations.

Increased Phospho-Y1604 ALK *as a Diagnostic Marker for Lung Cancer*

Given that all of the 10 lung adenocarcinoma specimens we examined showed an increase in the expression of phospho-Y1604 ALK compared with normal lung sections, we investigated the expression level of the endogenous phospho-Y1604 ALK in 13 different lung cancer cell lines and in 5 other cancer cell lines known to express total and phospho-Y1604 ALK as control. As shown in Figure 2*A*, the

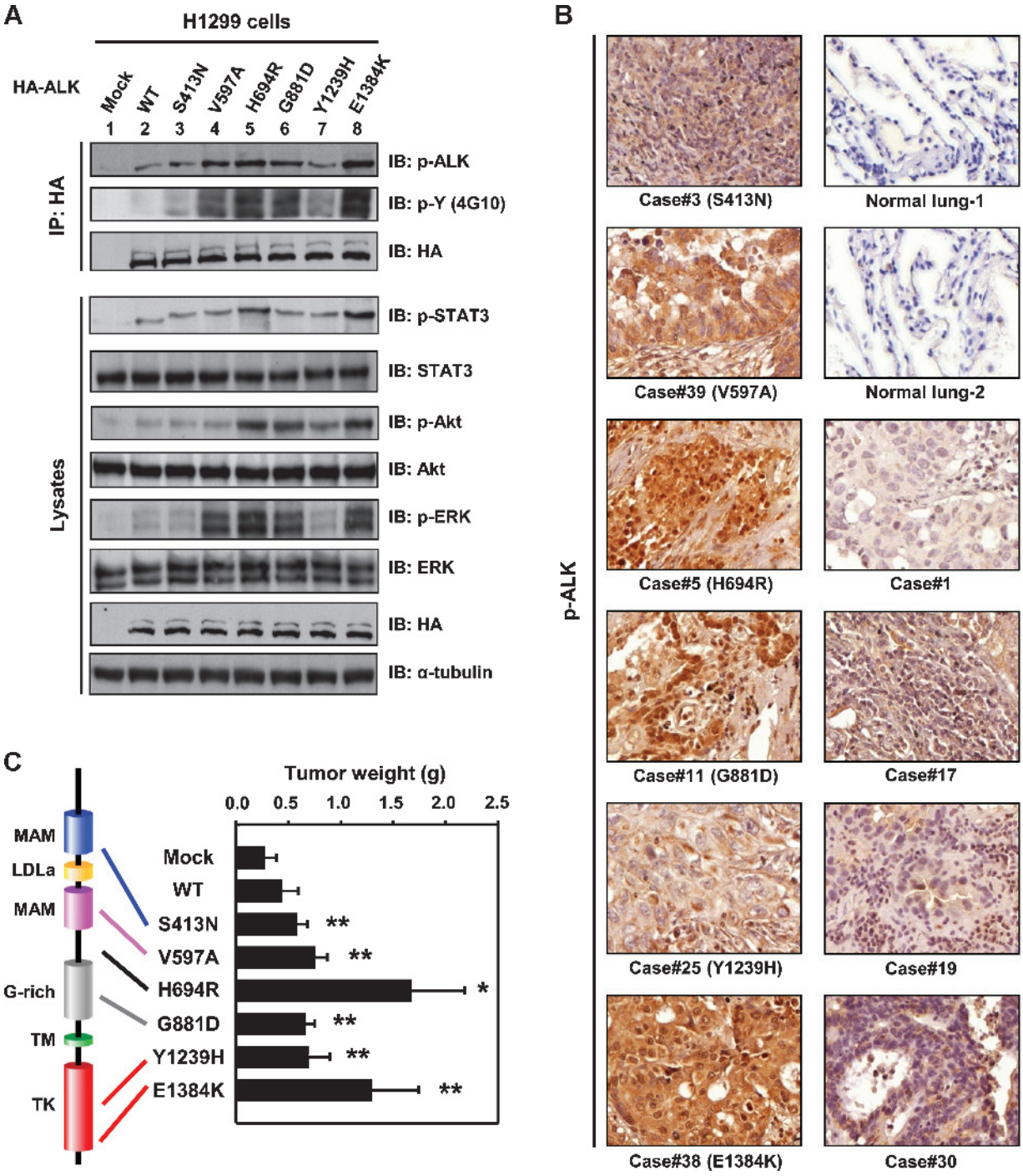

Figure 1. ALK mutations increased phosphorylation of ALK signaling pathways and tumorigenicity. (A) Expression of phospho-Y1604 ALK, overall tyrosine phosphorylation of ALK and downstream efforts of STAT3, AKT, and ERK in ALK transfectants of H1299 cells using IP (anti-HA antibody) and Western blot analyses. The α-tubulin served as an internal control. (B) IHC analysis of phospho-Y1604 ALK expression in human lung tissue sections of six lung cancer cases with ALK mutations, four lung cancer cases without ALK mutations, and two normal lung samples. (C) *In vivo* xenograft assay for tumorigenesis of ALK transfectants in H1299 cells (five mice per group; $*P < .05$, $**P < .01$). Identified ALK mutations are annotated along the schematic diagram of ALK protein structure containing two meprin/A5-protein/PTPmu (MAM) domains, one LDL receptor class A (LDLA) domain, one glycine-rich region, a transmembrane domain (TM), and a cytoplasmic tyrosine kinase (TK) domain.

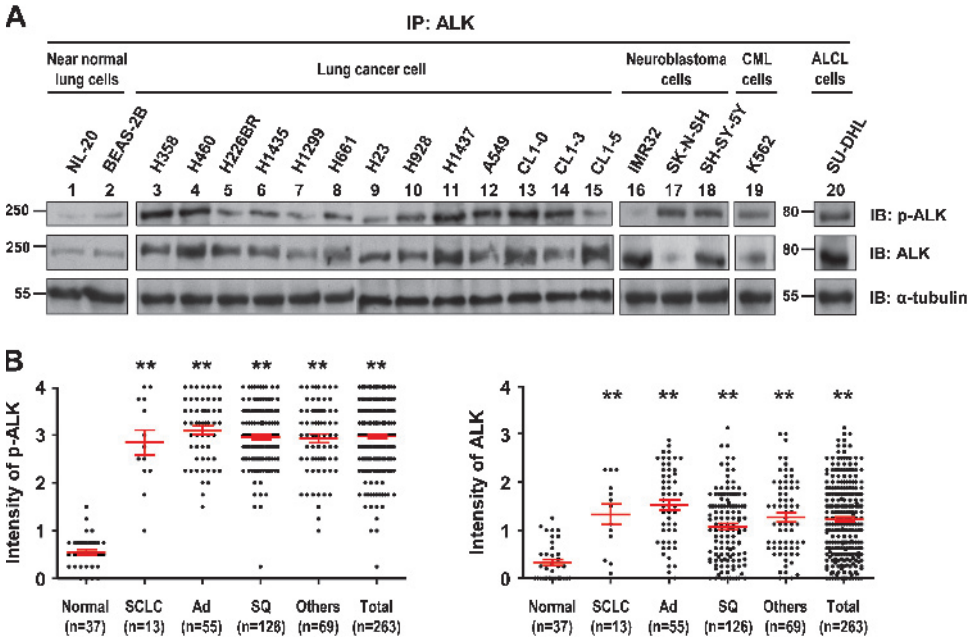

Figure 2. Hyperphosphorylation of ALK in lung cancer. (A) Phospho-Y1604 ALK expression in lung cancer cell lines and near-normal bronchial epithelial cells. The lysates of 13 lung cancer cell lines and 2 near-normal bronchial epithelial cells lines as indicated were treated with IP assay using anti-ALK antibody and subjected to Western blot analysis for detection of total and phospho-Y1604 ALK protein expression. K562 (NPM-ALK$^-$), SU-DHL (NPM-ALK$^+$), and three neuroblastoma cells IMR32 (wild-type ALK), SH-SY-5Y (F1174L mutant ALK), and SK-N-SH (F1174L mutant ALK) served as antibody controls. The α-tubulin was used as an internal control. (B) IHC analysis of phospho-Y1604 and total ALK expression in normal lung and lung cancer specimens. Tissue arrays contained most subtypes of lung cancer (total cases = 263) including SCLCs, adenocarcinomas (Ad), squamous cell carcinomas (SQ), and other subtypes. The red lines displayed the intensity by mean ± SD. $^{**}P < .01$.

expression level of phospho-Y1604 ALK in all of the 13 lung cancer cell lines was higher than that in the 2 immortalized near-normal bronchial epithelial cells. We next examined the expression of endogenous phospho-Y1604 ALK in clinical specimens using IHC staining conducted on 5 lung cancer tissue arrays with a total of 37 normal lung tissues and 263 lung cancer tissues including 13 small cell lung cancers, 55 adenocarcinomas, 126 squamous cell carcinomas, and 69 other subtypes of lung cancers. The staining intensity was blindly and independently evaluated by two pathologists using a semiquantitative score ranging from 0 to 4, with 4 indicative of the highest intensity and 0 indicative of lacking signal. The representative specimens assigned a score of 0, 1, 2, 3, or 4 from each tissue array are illustrated in Figure W2. As shown in Figure 2*B*, across all types of lung cancers and stages, tumors scored significantly higher than nonneoplastic lung tissues, with a mean score of 2.9684 ± 0.6852 *versus* 0.554 ± 0.3340 ($P < .001$), respectively. The diagnostic sensitivity of IHC score greater than 1 and greater than 2 for lung cancers reached 99.6% and 92.8%, respectively. The same specimens were also scored with IHC staining of total ALK. Regardless of cancer subtypes and stages, the sensitivity of cancer detection for total ALK score greater than 1 and greater than 2 was significantly lower and reached only 61.59% (162/263) and 18.3% (48/263), respectively. Statistical analysis revealed lack of correlation between the intensity of phospho-Y1604 and that of total ALK in lung cancer samples ($P = .4449$; Table W3). Altogether, our results demonstrated that activation of ALK played an important role not only in adenocarcinoma but also in other types of lung cancers. More importantly, the increased expression of phospho-Y1604 ALK could be an early step in lung cancer development and potentially be a useful diagnostic marker for lung cancer.

Tumorigenic Signaling of H694R *and* E1384K *Mutations in Mouse Xenograft Models*

To further explore molecular mechanism underlying ALK mutations-mediated tumorigenesis, we selected H694R and E1384K ALK mutants for further studies because they demonstrated the highest ability to promote growth of the xenograft tumors. To confirm the results of H694R and E1384K mutants obtained in H1299 cells (Figure 1*A*), we repeated the studies by overexpressing H694R and E1384K in NIH3T3 cells, which is another cell line commonly used to assess oncogenic property of ALK alterations in non–lung cancer genetic background [23,29]. Consistent with the results of the H1299 cell model, overexpression of H694R or E1384K mutant in NIH3T3 cells significantly enhanced the kinase activity and the downstream signaling of ALK as compared with wild-type counterpart (Figure 3*A*).

The enhanced tyrosine kinase activity of H694R and of E1384K was further validated by *in vitro* kinase assay (Figure W3). In addition, we also examined the effects of H694R and E1384K mutations on protein stability and subcellular localization of ALK protein. Our results showed that wild-type, H694R, or E1384K mutant ALK proteins shared a half-life of approximately 3.5 hours after cycloheximide treatment and uniform cytoplasmic localization (Figure W4).

Next, we examined the oncogenic effects of H694R and E1384K mutations in H1299 and NIH3T3 stable cells. In comparison with mock control, overexpression of wild-type ALK only slightly enhanced

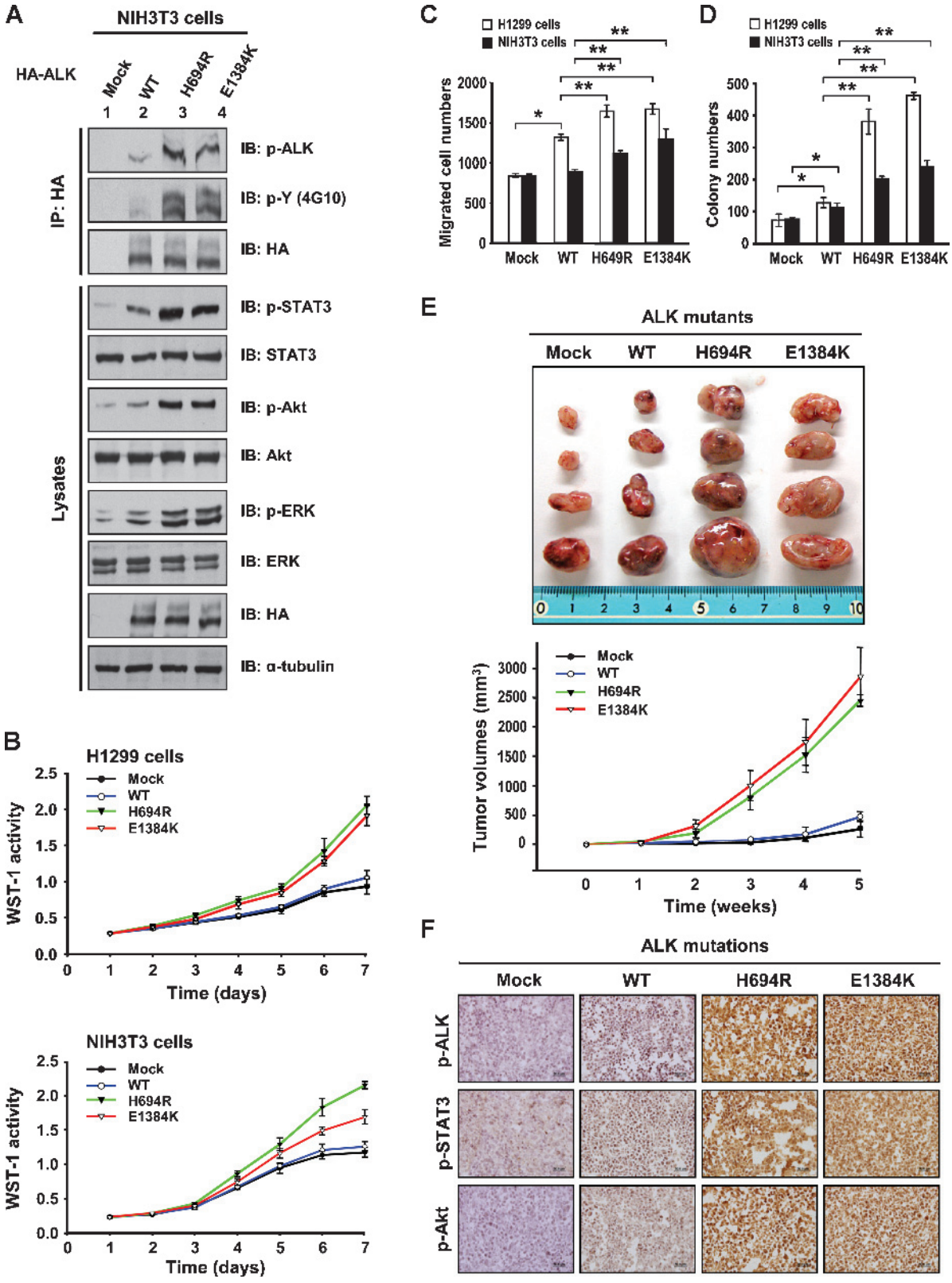

Figure 3. Transforming activity of ALK H694R and E1384K mutations in H1299 and NIH3T3 cells. (A) Expression of phospho-Y1604 ALK, overall tyrosine phosphorylation of ALK, and downstream efforts of STAT3, AKT, and ERK in ALK transfectants of NIH3T3 cells using IP (anti-HA antibody) and Western blot analyses. The α-tubulin served as an internal control. Oncogenic effects of H694R and E1384K transfectants of NIH3T3 and H1299 cells in cell proliferation (B), cell migration (C), and AIG (D). (E) *In vivo* tumor formation capability of H694R and E1384K transfectants of H1299. The xenografted tumor volume is displayed in the photograph (top panel) and in tumor growth curves (bottom panel) after 5 weeks of subcutaneous inoculation (four mice per group). (F) IHC analysis of phospho-Y1604 ALK and ALK downstream signaling effectors p-STAT3 and p-AKT in xenografted tumor sections of H694R and E1384K transfectants of H1299. Scale bars, 50 μm. Data are shown as mean ± SD. *$P < .01$. **$P < .001$.

proliferative activity after 7 days and showed a significant increase in cell migration assay and anchorage-independent growth (AIG) in soft agar. In contrast, the expression of H694R or E1384K mutant ALK exhibited significantly increased oncogenic properties in all three assays compared with the wild-type counterpart (Figure 3, *B-D*).

To validate the oncogenic property of H694R and E1384K mutants *in vivo*, H1299 cells were injected into nude mice, and the growth curve of the xenografted tumors was measured. Again, cells stably expressing wild-type ALK had slightly increased tumor volume 5 weeks after injection. In contrast, the tumors expressing H694R or E1384K showed a significant upshift in the growth curve as early as 2 weeks after injection, and the difference continued to expand throughout the assay period (Figure 3*E*). No significant difference in the growth curve was noted between the tumors with ALK mutants.

To correlate the tumorigenic ability of ALK mutations with their kinase activities, we performed IHC staining on sections from xenografted tumors using antibodies against phospho-Y1604 ALK, phospho-STAT3, and phospho-AKT. Our results consistently showed that the ALK activity, as measured by the phosphorylated proteins of ALK, STAT3, and AKT, only marginally increased in tumors expressing wild-type ALK but was significantly upregulated in H694R and E1384K mutant-expressing xenografted tumors (Figure 3*F*). Taken together, our findings illustrated that H694R and E1384K mutations led to constitutive activation of ALK activity and its downstream effectors STAT3, AKT, and ERK, which, in turn, promoted tumorigenesis without altering ALK protein stability or subcellular localization.

H694R *and* E1384K *Mutation-Bearing Tumors Sensitive to Treatment of ALK Inhibitors*

To investigate whether small-molecule ALK inhibitor could suppress ALK mutation-mediated tumorigenic properties, cells or xenografted tumors expressing wild-type, H694R, or E1384K mutant ALKs were treated with WHI-P154, which could repress kinase activity of ALK [23,41,42]. The results demonstrated that WHI-P154 treatment showed a dose-dependent inhibition of growth in cells expressing wild-type or mutant ALKs (Figure 4*A*). Analytically, the half-maximal cell growth-inhibitory concentration (IC_{50}) of H694R and E1384K mutations were 2.28- to 2.86-folds lower than that of wild-type. It was concluded that cells expressing H694R or E1384K mutant ALK were even more sensitive to inhibitory effect of WHI-P154 than cells expressing wild-type ALK (Table W4).

The effects of WHI-P154 on cell migration and AIG were also examined in H1299 stable cells. Consistently, WHI-P154 treatments resulted in a profound inhibition of cell migration and AIG in H1299 expressing either wild-type or mutant ALKs compared with DMSO control (Figure 4*A*). Given the stronger effects of mutant ALK than wild-type ALK on the cell migration and AIG, it was no surprise that WHI-P154 inhibited the mutant ALK more than the wild-type. Notably, the oncogenic effects of mutant ALK became comparable to the wild-type ALK in both assays after WHI-P154 treatment, indicating the ALK inhibitor reversed the property of mutant ALK back to the basal level. As shown in Figure 4*B*, WHI-P154 treatment repressed phosphorylation of ALK Y1604 in a dose-dependent manner, suggesting that WHI-P154 inhibited the aforementioned oncogenic effects of ALK by suppressing its kinase activity.

Because the WHI-P154 was recently reported to be an inhibitor of JAK3/STAT3 as well, to further validate the therapeutic efficacy of ALK inhibitor in mutations-induced oncogenesis, a more specific ALK inhibitor NVP-TAE684 was included [36]. Similarly, TAE684 treatment efficiently inhibited the cell proliferation and phospho-Y1604 ALK expression of H694R or E1384K mutant ALK, but also to a degree higher than that of wild-type ALK (Figure 5, *A* and *B*). Altogether, our results showed that oncogenic ALK mutations could be a potential therapeutic target and ALK inhibitors could be therapeutic agents in lung adenocarcinomas.

Inhibition of Tumor Metastasis and Improvement of Survival by WHI-P154

To evaluate if the inhibitory effect of WHI-P154 on the oncogenic property of mutant ALKs at the molecular level could be translated into improved clinical outcomes, we next examined two important parameters, namely, pulmonary metastasis and animal survival, using an *in vivo* subcutaneous xenograft mouse model. When the xenografted tumors grew to volumes around 20 to 50 mm^3, mice were randomly divided into two groups and treated with WHI-P154 or DMSO daily. As expected, WHI-P154–treated H694R- or E1384K-bearing tumors showed a significant reduction in their growth compared with DMSO-treated tumors (Figure 4*C*). In agreement with the reduction in tumor growth, a significant decrease in the expression of phospho-Y1604 ALK was detected in WHI-P154–treated tumors compared with DMSO-treated counterparts (Figure 4*D*). The therapeutic efficacy of the ALK inhibitor on the xenograft mouse model was further validated with TAE684. Consistently, TAE684 treatment repressed H694R- and E1384K-induced tumor growth compared with DMSO control (Figure 5*C*).

To investigate if the ALK inhibitors prevented lung metastasis, H1299 cells coexpressing GFP/H694R or GFP/E1384K mutant ALK were injected through the tail veins, and systemic metastases were examined. Both H694R- and E1384K-expressing cells showed higher capability in lung metastasis compared with wild-type and mock control. More importantly, WHI-P154 treatment significantly suppressed lung metastasis in mice injected with H1299 cells expressing mutant ALK proteins (Figure 4*E*). Furthermore, mice with metastatic tumors expressing H694R or E1384K mutations started to die prematurely from day 60 (Figure 4*F*). Particularly, mice injected with E1384K-bearing cells were associated with a high metastatic rate and poor survival ($P = .0246$) compared with mice bearing cells expressing wild-type ALK or mock control. In contrast, WHI-P154 treatment rescued mice injected with cells expressing H694R or E1384K mutant ALK from premature death and reversed the survival back to the level of the control mice (Figure 4*F*). Taken together, in this study, we demonstrated that ALK mutations resulted in constitutive activation of ALK activity and its downstream oncogenic signaling, which, in turn, led to tumorigenesis. Targeting the aberrant ALK signaling pathway activated by mutations with ALK inhibitors not only suppressed tumorigenesis and metastasis but also prolonged the survival of mice bearing tumors induced by mutant ALK.

Discussion

In this study, we provided evidence that ALK was involved in the pathogenesis of lung cancers. Our data showed that ALK could be aberrantly activated not only through fusion with other partner genes but also through other mechanisms such as somatic point mutations. Therefore, ALK alterations could occur through defects in heterogeneous regulatory mechanisms. The long-term increase of phospho-Y1604 ALK either by fusion or by point mutations resulted in constitutive activation of its downstream STAT3, AKT and ERK signaling pathways and subsequent tumor formation and progression. Treatment

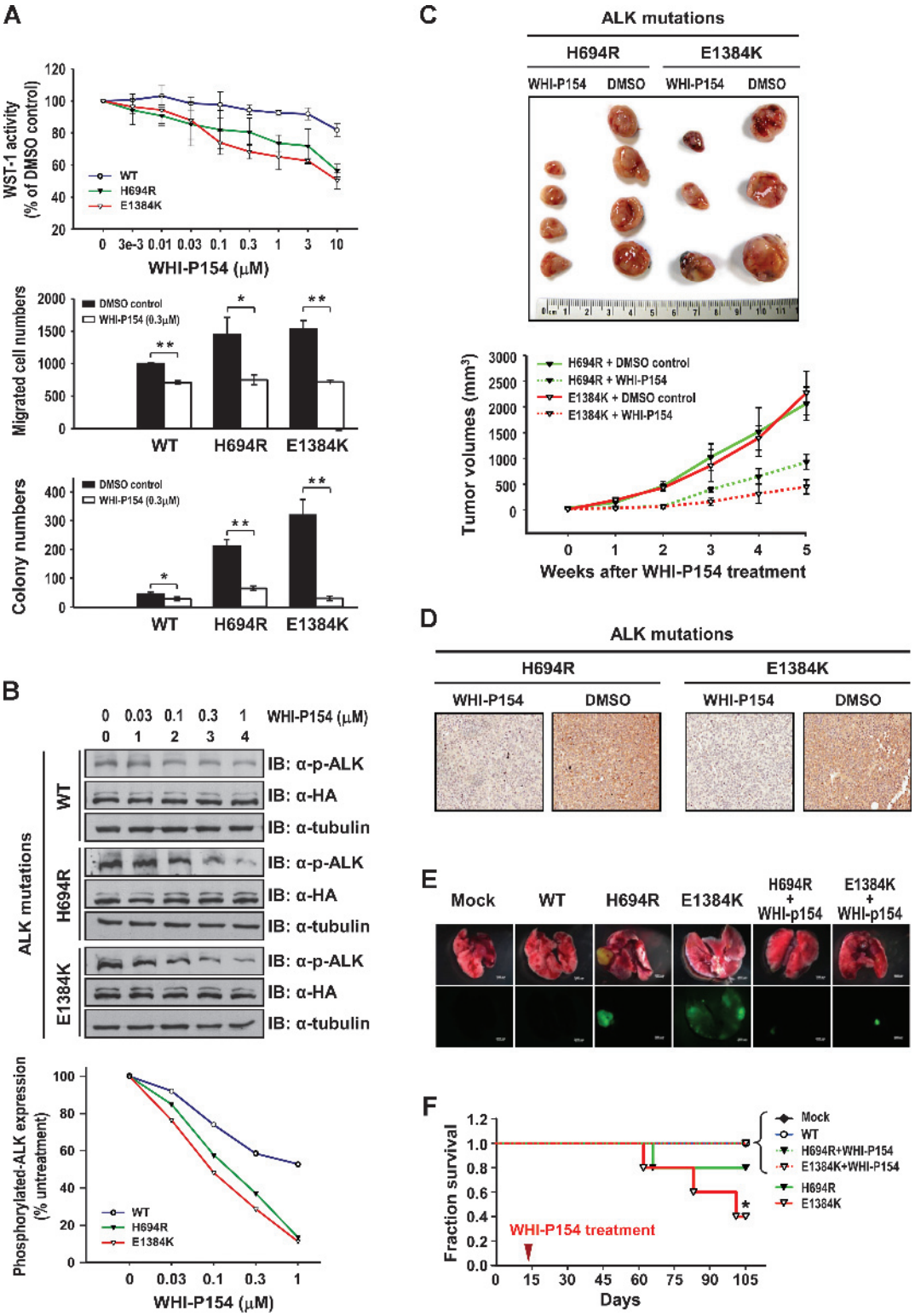

Figure 4. Therapeutic effects of ALK inhibitor WHI-P154 on H694R- and E1384K-mediated tumorigenesis of H1299 transfectants. (A) Effects of WHI-P154 on cell growth (top panel), cell migration (middle panel), and AIG (bottom panel) expressing wild-type, H694R, or E1384K mutant ALKs. (B) The dosage effects of WHI-P154 on phospho-Y1604 ALK expression of wild-type, H694R, and E1384K ALKs by Western blot analysis (top panel). The quantitative intensity of phospho-Y1604 ALK expression is shown in the bottom panel compared with the internal control expression of α-tubulin. (C) The suppressive effects of WHI-P154 on H694R- and E1384K-induced tumor *in vivo*. Photographs and the tumor growth curves are shown in the top and bottom panels, respectively (four mice per group). (D) IHC analysis of phospho-Y1604 ALK expression in xenografted tumor sections of H694R and E1384K after WHI-P154 treatment. (E and F) The suppressive effects of WHI-P154 on H694R- and E1384K-mediated lung metastasis after tail vein injections of GFP-labeling H1299 transfectants. The systemic lung metastasis models are visualized in macroscopic and fluorescent views of lung images (E) and survival analysis are shown in F (five mice per group). Scale bars, 2000 μm.

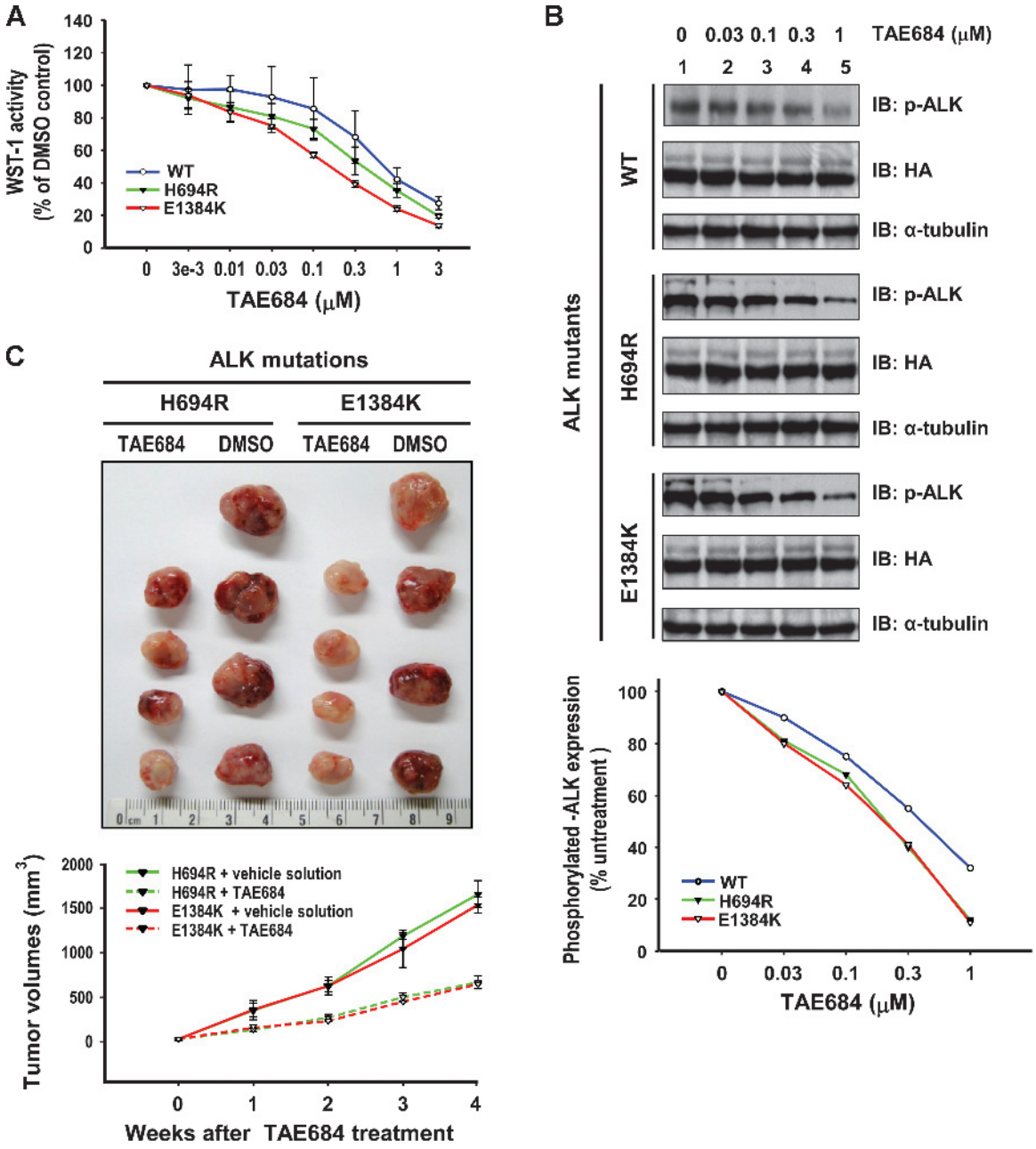

Figure 5. Therapeutic effects of ALK inhibitor TAE684 on H694R- and E1384K-mediated tumorigenesis of H1299 transfectants. (A) Dosage effects of TAE684 on H694R- and E1384K-induced cell proliferation measured with WST-1 activity. (B) Dosage effects of TAE684 on phospho-Y1604 ALK expression of wild-type, H694R, and E1384K transfectants by Western blot analysis (top panel). Quantitative results of phospho-Y1604 ALK intensity are also (bottom panel). (C) Suppressive effects of TAE684 on H694R- and E1384K-induced tumors *in vivo*. Photographs and tumor growth curves are shown in the top and bottom panels, respectively (four mice per group).

of ALK inhibitors on the xenografted tumors could also inhibit growth and metastasis of these tumors. Our results further indicated that ALK activation contributed not only to the early stage of tumorigenesis but also to the continuous growth and/or metastasis of the tumors. Therefore, ALK alterations in the form of aberrant increase in Y1604 phosphorylation or point mutations could potentially serve as a diagnosis biomarker and therapeutic target for lung cancer.

Previous studies showed that endogenous ALK protein expression was difficult to detect in lung tissues by IHC [43,44]; however, we were able to detect endogenous ALK expression in lung cancer sections using the antibody produced by Epitomics. After extensively screening most of the commercially available ALK antibodies, we found that, by IHC or by Western blot analyses, the signals of ALK recognized by the Epitomics antibody were consistently stronger than those obtained by DAKO ALK antibody commonly used in previous studies [45] (Figure W5, *B* and *C*). The specificity of this ALK antibody was also validated in this study using IHC assay and Western blot analyses. As shown in Figure W5*A*, both ALCL and rhabdomyosarcoma reported to have higher ALK expression indeed were showed to have strong total ALK staining intensity compared with normal lymph node using Epitomics ALK antibody [46]. The same specimens were also examined for phospho-ALK expression. Again, ALCL tissue sections showed strong

phospho-ALK signal, and the rhabdomyosarcoma tissue sections seemed more variable but showed a clear trend of lower intensity. In addition, on the Western blot, the Epitomics antibody recognized a band with an appropriate molecular weight of ALK (Figure W5*C*).

Mutations in *ALK* we identified showed differential effects on the tumorigenesis. Therefore, it may be of great significance for therapeutic implications to correlate these mutations with their oncogenic functions based on protein structure information. However, given that ALK is a 250-kd protein with structural information only available for the tyrosine kinase domain, it may be difficult to fully address this issue. We directly assessed the tumorigenic property of these six identified ALK mutations by analyzing their kinase activities and *in vivo* tumor formation capabilities in nude mice. As shown in our results, H694R and E1384K mutations possessed the strongest oncogenic property. Because H694R mutation is located outside the kinase domain, it is difficult to predict the impact of this mutation on the structure of the kinase domain. In contrast, E1384K mutation is localized in the kinase domain and resides within the alpha-helix (αI) near-activation loop [47]. The nearest amino acid residue on ALK structure is R1231 positioned at another alpha-helix (αE). We speculate that E1384K mutation alters the electronegative 1384 glutamic acid (E) residue to an electropositive lysine (K) residue and may disrupt the interaction between these two alpha helices through electrostatic repulsive forces and result in conformational change and increased kinase activity.

In addition to H694R and E1384K mutations, the four remaining *ALK* mutations also showed a significant increase in their ability to promote tumorigenesis *in vivo* compared with wild-type *ALK*, indicating that these *ALK* mutations could also be gain-of-function driver mutations. However, only V597A and G881D increased phospho-Y1604 ALK expression, but S413N and Y1239H mutations did not. The H694R and E1384K mutations could activate STAT3, AKT, and ERK; V597A only activated ERK, and G881D activated AKT and ERK. These findings indicated that each individual ALK mutation selectively targeted specific downstream mediators. Our mutations behaved similarly to the F1174L ALK mutation previously identified in neuroblastoma. Overexpression of F1174L mutant ALK significantly increased phospho-Y1604 ALK, and phosphorylation of downstream targets STAT3 and AKT, but ERK phosphorylation was not affected [32]. These results suggest that *ALK* mutations may mediate tumorigenesis through increased ALK activity, noncanonical phosphorylation sites and/or kinase activity–independent manner such as ligand-binding activation or acquiring mutation-specific protein interactions. In our preliminary data, transient expression of ligand pleiotrophin in or addition of recombinant pleiotrophin to H1299 cells expressing mutant ALK did not show a significant change in the phosphorylation status of Y1604.

In our study, we selected NIH3T3 (normal mouse fibroblast) and H1299 (lung cancer cell carried heterozygous N-*ras* Q61K mutation) cells to evaluate alteration in kinase activity; downstream activation of STAT3, AKT, and ERK effectors; and tumorigenic effects by H694R and E1384K mutations. Our results suggested that host cell genetic background such as N-*ras* Q61K mutation in H1299 is unlikely to participate in ALK mutation–mediated tumorigenesis. First, the expression of mutant ALKs in H1299 and NIH3T3 showed a similar activation of downstream ALK signaling and oncogenic effects. Second, overexpression of wild-type and mutant ALKs increased phospho-Y1604 ALK, phospho-STAT3, phospho-AKT, and phospho-ERK, which failed to be activated by the overexpression of the kinase-dead K1150R mutant (equivalent to the K210R NPM-ALK mutant) or was repressed after TAE684 treatment (Figure W6, *A* and *B*). Finally, treatment of ALK-specific shRNA suppressed H694R and E1384K mutations–mediated cell growth (Figure W7). These results indicate that ALK mutations conferred a driver function to stimulate STAT3, AKT, and ERK in a kinase activity–dependent manner and worked independently of the active GTP-bound state of N-*ras* Q61K mutation in lung cancer.

Because WHI-P154 is an ALK inhibitor that may also target STAT3, we therefore treated H694R- and E1384K-bearing H1299 cells with the more specific ALK inhibitor NVP-TAE684. As shown in Figure 5, *A* and *C*, TAE684 treatment demonstrated similar therapeutic benefits to that by WHI-P154 treatment both *in vitro* and *in vivo*. In addition, the increased sensitivity of H694R and E1384K mutations to specific shRNA knockdown compared with the wild-type counterpart (48% and 52% *vs* 27%; Figure W7) and the ALK inhibitor WHI-P154 or NVP-TAE684 in various functional assays showed that the acquired somatic mutations not only rendered lung cancer cells addictive to constitutive ALK activity to gain advantage of growth and survival but also served as a suitable target for lung adenocarcinoma treatment. In addition, although molecular mechanisms of suppressing cancer metastasis by WHI-P154 remain to be determined, prolonged survival of mice injected with H694R- and E1384K-bearing cells clearly suggested the therapeutic benefits of ALK inhibitor in lung cancer.

To further delineate the potential role of ALK somatic alterations as a diagnostic biomarker and predictor of therapeutic benefits for lung cancer, several tasks need to be conducted in the near future. First, phosphorylation status and mutations of ALK should be closely examined in larger cohorts and across different ethnic populations in relations to various risk factors for potential disparities. Second, efforts should be directed to study the etiological mechanisms of aberrantly increased ALK phosphorylation and mutations in lung cancer that eventually alter protein structures, enhance ALK tyrosine kinase activity, and constitutively activate downstream oncogenic signaling pathways. These efforts will benefit not only our understanding of the heterogeneous mechanisms ALK signaling induces tumor formation but also the clinical management of ALK-mutated lung cancer patients. Finally, the ALK inhibitor WHI-P154 inhibited tumor progression and prolonged survival in mouse lung cancer models mainly through the suppression of the canonical ALK pathway; however, it also "off target" to suppress STAT3 pathway in *ALK* mutation-bearing cells. Our results raise a possibility of a combinatorial therapy for lung cancers composed of other more specific ALK inhibitors with WHI-P154 or inhibitor targeting ALK downstream mediators for a synergistic benefit. This study should facilitate the development of new ALK inhibitors for personalized lung cancer treatment.

Acknowledgments

The authors thank Yih-Leong Chang, Chen-Tu Wu, and Yung-Chie Lee of the Departments of Pathology and of Surgery and Traumatology, College of Medicine, National Taiwan University, for their technical and material support; and the National RNAi Core Facility from the National Research Program for Genomic Medicine, National Science Council, Taiwan, for providing the shRNA.

References

[1] World Health Organization. *Cancer*. Geneva, Switzerland: World Health Organization. Available at: http://www.who.int/mediacentre/factsheets/fs297/en/. Fact sheet N°297, February 2011.

[2] Ladanyi M and Pao W (2008). Lung adenocarcinoma: guiding EGFR-targeted therapy and beyond. *Mod Pathol* **21**(suppl 2), S16–S22.

[3] Ma PC, Jagadeeswaran R, Jagadeesh S, Tretiakova MS, Nallasura V, Fox EA, Hansen M, Schaefer E, Naoki K, Lader A, et al. (2005). Functional expression and mutations of c-Met and its therapeutic inhibition with SU11274 and small interfering RNA in non–small cell lung cancer. *Cancer Res* **65**, 1479–1488.

[4] Stephens P, Hunter C, Bignell G, Edkins S, Davies H, Teague J, Stevens C, O'Meara S, Smith R, Parker A, et al. (2004). Lung cancer: intragenic ERBB2 kinase mutations in tumours. *Nature* **431**, 525–526.

[5] Paez JG, Janne PA, Lee JC, Tracy S, Greulich H, Gabriel S, Herman P, Kaye FJ, Lindeman N, Boggon TJ, et al. (2004). EGFR mutations in lung cancer: correlation with clinical response to gefitinib therapy. *Science* **304**, 1497–1500.

[6] Lynch TJ, Bell DW, Sordella R, Gurubhagavatula S, Okimoto RA, Brannigan BW, Harris PL, Haserlat SM, Supko JG, Haluska FG, et al. (2004). Activating mutations in the epidermal growth factor receptor underlying responsiveness of non–small-cell lung cancer to gefitinib. *N Engl J Med* **350**, 2129–2139.

[7] Takahashi T, Nau MM, Chiba I, Birrer MJ, Rosenberg RK, Vinocour M, Levitt M, Pass H, Gazdar AF, and Minna JD (1989). p53: a frequent target for genetic abnormalities in lung cancer. *Science* **246**, 491–494.

[8] Santos E, Martin-Zanca D, Reddy EP, Pierotti MA, Della Porta G, and Barbacid M (1984). Malignant activation of a K-*ras* oncogene in lung carcinoma but not in normal tissue of the same patient. *Science* **223**, 661–664.

[9] Samuels Y and Velculescu VE (2004). Oncogenic mutations of PIK3CA in human cancers. *Cell Cycle* **3**, 1221–1224.

[10] Samuels Y, Wang Z, Bardelli A, Silliman N, Ptak J, Szabo S, Yan H, Gazdar A, Powell SM, Riggins GJ, et al. (2004). High frequency of mutations of the *PIK3-CA* gene in human cancers. *Science* **304**, 554.

[11] Naoki K, Chen TH, Richards WG, Sugarbaker DJ, and Meyerson M (2002). Missense mutations of the *BRAF* gene in human lung adenocarcinoma. *Cancer Res* **62**, 7001–7003.

[12] Brose MS, Volpe P, Feldman M, Kumar M, Rishi I, Gerrero R, Einhorn E, Herlyn M, Minna J, Nicholson A, et al. (2002). *BRAF* and *RAS* mutations in human lung cancer and melanoma. *Cancer Res* **62**, 6997–7000.

[13] Sanchez-Cespedes M, Parrella P, Esteller M, Nomoto S, Trink B, Engles JM, Westra WH, Herman JG, and Sidransky D (2002). Inactivation of LKB1/STK11 is a common event in adenocarcinomas of the lung. *Cancer Res* **62**, 3659–3662.

[14] Subramanian J and Govindan R (2008). Molecular genetics of lung cancer in people who have never smoked. *Lancet Oncol* **9**, 676–682.

[15] Sun S, Schiller JH, and Gazdar AF (2007). Lung cancer in never smokers—a different disease. *Nat Rev Cancer* **7**, 778–790.

[16] Herbst RS, Heymach JV, and Lippman SM (2008). Lung cancer. *N Engl J Med* **359**, 1367–1380.

[17] Sun S, Schiller JH, Spinola M, and Minna JD (2007). New molecularly targeted therapies for lung cancer. *J Clin Invest* **117**, 2740–2750.

[18] Jemal A, Siegel R, Ward E, Hao Y, Xu J, and Thun MJ (2009). Cancer statistics, 2009. *CA Cancer J Clin* **59**, 225–249.

[19] Fischer P, Nacheva E, Mason DY, Sherrington PD, Hoyle C, Hayhoe FG, and Karpas A (1988). A Ki-1 (CD30)–positive human cell line (Karpas 299) established from a high-grade non–Hodgkin's lymphoma, showing a 2;5 translocation and rearrangement of the T-cell receptor β-chain gene. *Blood* **72**, 234–240.

[20] Morris SW, Kirstein MN, Valentine MB, Dittmer KG, Shapiro DN, Saltman DL, and Look AT (1994). Fusion of a kinase gene, *ALK*, to a nucleolar protein gene, *NPM*, in non–Hodgkin's lymphoma. *Science* **263**, 1281–1284.

[21] Chiarle R, Voena C, Ambrogio C, Piva R, and Inghirami G (2008). The anaplastic lymphoma kinase in the pathogenesis of cancer. *Nat Rev Cancer* **8**, 11–23.

[22] Horn L and Pao W (2009). EML4-ALK: honing in on a new target in non–small-cell lung cancer. *J Clin Oncol* **27**, 4232–4235.

[23] Soda M, Choi YL, Enomoto M, Takada S, Yamashita Y, Ishikawa S, Fujiwara S, Watanabe H, Kurashina K, Hatanaka H, et al. (2007). Identification of the transforming *EML4-ALK* fusion gene in non–small-cell lung cancer. *Nature* **448**, 561–566.

[24] Soda M, Takada S, Takeuchi K, Choi YL, Enomoto M, Ueno T, Haruta H, Hamada T, Yamashita Y, Ishikawa Y, et al. (2008). A mouse model for EML4-ALK–positive lung cancer. *Proc Natl Acad Sci USA* **105**, 19893–19897.

[25] Li Y, Ye X, Liu J, Zha J, and Pei L (2011). Evaluation of EML4-ALK fusion proteins in non–small cell lung cancer using small molecule inhibitors. *Neoplasia* **13**, 1–11.

[26] Ding L, Getz G, Wheeler DA, Mardis ER, McLellan MD, Cibulskis K, Sougnez C, Greulich H, Muzny DM, Morgan MB, et al. (2008). Somatic mutations affect key pathways in lung adenocarcinoma. *Nature* **455**, 1069–1075.

[27] Choi YL, Soda M, Yamashita Y, Ueno T, Takashima J, Nakajima T, Yatabe Y, Takeuchi K, Hamada T, Haruta H, et al. (2010). *EML4-ALK* mutations in lung cancer that confer resistance to ALK inhibitors. *N Engl J Med* **363**, 1734–1739.

[28] Palmer RH, Vernersson E, Grabbe C, and Hallberg B (2009). Anaplastic lymphoma kinase: signalling in development and disease. *Biochem J* **420**, 345–361.

[29] Chen Y, Takita J, Choi YL, Kato M, Ohira M, Sanada M, Wang L, Soda M, Kikuchi A, Igarashi T, et al. (2008). Oncogenic mutations of ALK kinase in neuroblastoma. *Nature* **455**, 971–974.

[30] Janoueix-Lerosey I, Lequin D, Brugieres L, Ribeiro A, de Pontual L, Combaret V, Raynal V, Puisieux A, Schleiermacher G, Pierron G, et al. (2008). Somatic and germline activating mutations of the ALK kinase receptor in neuroblastoma. *Nature* **455**, 967–970.

[31] Mosse YP, Laudenslager M, Longo L, Cole KA, Wood A, Attiyeh EF, Laquaglia MJ, Sennett R, Lynch JE, Perri P, et al. (2008). Identification of *ALK* as a major familial neuroblastoma predisposition gene. *Nature* **455**, 930–935.

[32] George RE, Sanda T, Hanna M, Frohling S, Luther W II, Zhang J, Ahn Y, Zhou W, London WB, McGrady P, et al. (2008). Activating mutations in *ALK* provide a therapeutic target in neuroblastoma. *Nature* **455**, 975–978.

[33] Tseng RC, Chang JW, Hsien FJ, Chang YH, Hsiao CF, Chen JT, Chen CY, Jou YS, and Wang YC (2005). Genomewide loss of heterozygosity and its clinical associations in non small cell lung cancer. *Int J Cancer* **117**, 241–247.

[34] Lamant L, Pulford K, Bischof D, Morris SW, Mason DY, Delsol G, and Mariame B (2000). Expression of the *ALK* tyrosine kinase gene in neuroblastoma. *Am J Pathol* **156**, 1711–1721.

[35] Marzec M, Kasprzycka M, Liu X, El-Salem M, Halasa K, Raghunath PN, Bucki R, Wlodarski P, and Wasik MA (2007). Oncogenic tyrosine kinase NPM/ALK induces activation of the rapamycin-sensitive mTOR signaling pathway. *Oncogene* **26**, 5606–5614.

[36] Galkin AV, Melnick JS, Kim S, Hood TL, Li N, Li L, Xia G, Steensma R, Chopiuk G, Jiang J, et al. (2007). Identification of NVP-TAE684, a potent, selective, and efficacious inhibitor of NPM-ALK. *Proc Natl Acad Sci USA* **104**, 270–275.

[37] Balsara BR and Testa JR (2002). Chromosomal imbalances in human lung cancer. *Oncogene* **21**, 6877–6883.

[38] Weir BA, Woo MS, Getz G, Perner S, Ding L, Beroukhim R, Lin WM, Province MA, Kraja A, Johnson LA, et al. (2007). Characterizing the cancer genome in lung adenocarcinoma. *Nature* **450**, 893–898.

[39] Yuan J, Ma J, Zheng H, Shi T, Sun W, Zhang Q, Lin D, Zhang K, He J, Mao Y, et al. (2008). Overexpression of OLC1, cigarette smoke, and human lung tumorigenesis. *J Natl Cancer Inst* **100**, 1592–1605.

[40] Tsai MF, Wang CC, Chang GC, Chen CY, Chen HY, Cheng CL, Yang YP, Wu CY, Shih FY, Liu CC, et al. (2006). A new tumor suppressor DnaJ-like heat shock protein, HLJ1, and survival of patients with non–small-cell lung carcinoma. *J Natl Cancer Inst* **98**, 825–838.

[41] Marzec M, Kasprzycka M, Ptasznik A, Wlodarski P, Zhang Q, Odum N, and Wasik MA (2005). Inhibition of ALK enzymatic activity in T-cell lymphoma cells induces apoptosis and suppresses proliferation and STAT3 phosphorylation independently of Jak3. *Lab Invest* **85**, 1544–1554.

[42] Colomba A, Courilleau D, Ramel D, Billadeau DD, Espinos E, Delsol G, Payrastre B, and Gaits-Iacovoni F (2008). Activation of Rac1 and the exchange factor Vav3 are involved in NPM-ALK signaling in anaplastic large cell lymphomas. *Oncogene* **27**, 2728–2736.

[43] Boland JM, Erdogan S, Vasmatzis G, Yang P, Tillmans LS, Johnson MR, Wang X, Peterson LM, Halling KC, Oliveira AM, et al. (2009). Anaplastic lymphoma kinase immunoreactivity correlates with *ALK* gene rearrangement and transcriptional up-regulation in non–small cell lung carcinomas. *Hum Pathol* **40**, 1152–1158.

[44] Martelli MP, Sozzi G, Hernandez L, Pettirossi V, Navarro A, Conte D, Gasparini P, Perrone F, Modena P, Pastorino U, et al. (2009). *EML4-ALK* rearrangement in non–small cell lung cancer and non–tumor lung tissues. *Am J Pathol* **174**, 661–670.

[45] Pulford K, Lamant L, Morris SW, Butler LH, Wood KM, Stroud D, Delsol G, and Mason DY (1997). Detection of anaplastic lymphoma kinase (ALK) and nucleolar protein nucleophosmin (NPM)-ALK proteins in normal and neoplastic cells with the monoclonal antibody ALK1. *Blood* **89**, 1394–1404.

[46] Corao DA, Biegel JA, Coffin CM, Barr FG, Wainwright LM, Ernst LM, Choi JK, Zhang PJ, and Pawel BR (2009). ALK expression in rhabdomyosarcomas: correlation with histologic subtype and fusion status. *Pediatr Dev Pathol* **12**, 275–283.

[47] Bossi RT, Saccardo MB, Ardini E, Menichincheri M, Rusconi L, Magnaghi P, Orsini P, Avanzi N, Borgia AL, Nesi M, et al. (2010). Crystal structures of anaplastic lymphoma kinase in complex with ATP competitive inhibitors. *Biochemistry* **49**, 6813–6825.

Table W1. ALK Mutants in 48 Lung Adenocarcinoma Patients.

Cases	Gender	Age (*y*)	Smoking	TNM	Stage	ALK Mutants
T01	M	64	Yes	T4	IIIB	
T02	F	68	No	T2	IB	
T03	M	65	Yes	T2	IIB	*G2145A, S413N*
T04	M	38	Yes	T2	IB	
T05	M	62	Yes	T2	IB	*A2988G, H694R*
T06	M	56	No	T2	IIIA	
T07	F	73	No	T2	IB	
T08	F	56	No	T1	IA	
T09	M	77	Yes	T3	IIB	
T10	M	73	Yes	T4	IIIB	
T11	M	56	Yes	T2	IB	*G3549A, G881D*
T12	M	77	Yes	T2	IIB	
T13	M	73	No	T2	IB	
T14	M	65	Yes	T2	IB	
T15	F	48	No	T2	IIIA	
T16	M	68	No	T2	IB	
T17	M	55	Yes	T2	IB	
T18	M	51	Yes	T2	IIB	
T19	F	76	No	T2	IIB	
T20	M	76	No	T2	IB	
T21	M	79	Yes	T3	IIIA	
T22	M	63	No	T4	IIIB	
T23	F	70	No	T1	IA	
T24	M	59	Yes	T3	IIIA	
T25	M	72	No	T2	IIIA	*T4622C, Y1239H*
T26	M	59	No	T2	IIB	
T27	M	72	No	T2	IB	
T28	M	59	Yes	T2	IIIA	
T29	M	40	No	T2	IB	
T30	M	69	No	T2	IB	
T31	M	57	No	T1	IA	
T32	M	62	No	T1	IA	
T33	F	51	No	T2	IB	
T34	F	60	No	T2	IIIA	
T35	F	64	No	T2	IB	
T36	F	70	No	T2	IIIA	
T37	F	63	No	T2	IIIA	
T38	F	68	No	T2	IIIA	*G5057A, E1384K*
T39	F	69	No	T2	IB	*T2697C, V597A*
T40	F	70	No	T2	IIIA	
T41	F	55	No	T2	IB	
T42	F	62	No	T2	IB	
T43	F	49	No	T3	IIIA	
T44	F	71	No	T1	IIA	
T45	F	67	No	T2	IB	
T46	M	48	Yes	T2	IIB	
T47	M	41	No	T2	IB	
T48	M	74	No	T2	IB	

Table W2. ALK Sequencing Primers.

ALK Primers	
Primer Name	Sequence
ALK01-1F	TCTGGAGATCAGGTGGAAGG
ALK01-1R	TGAACAGCTCGCTGAGAT
ALK01-2F	CCTCGCTCTTCCGTGTCTAC
ALK01-2R	AACACTAAATCCCGGCACAC
ALK02ex-F	TCAGGGTCCTGAGGTCAACT
ALK02ex-R	ATAGGGAGCTGAGGGAATGC
ALK03ex-F	TGAAGGCCAACCTCCTAGTG
ALK03ex-R	CCAAGAAGCCATGGAAAGTC
ALK04ex-F	GTCCACCTGCATCAGGCTAT
ALK04ex-R	GAAGTCAGAGGGACCCACAA
ALK05ex-F	AAAAGGAATGCCAGTGGTGAG
ALK05ex-R	CCAAACATGGTTGCAGGTTA
ALK06ex-F	AGGGAACATGGACCACTCTGCTG
ALK06ex-R	TGGGCATAGAGGACTTCCAATGTCACA
ALK07ex-F	TTGGGGGCTTCTCTTCATTA
ALK07ex-R	GAAAGCCCAAGGTGTGAAGA
ALK08ex-F	AGGTGGGCTTTCTTCTCCAT
ALK08ex-R	AGAGGTGGCCCTCTTGTTCT
ALK09ex-F	TCTTGGTGAGACAGGTGGTG
ALK09ex-R	GAGAAGGGTATTGGGGGAGA
ALK11_10ex-F	GGGATTAGCGAGCCTTTTTC
ALK11_10ex-R	ACAGCTCCCCACCCTAAAGA
ALK12ex-F	CATCTTGGATGGAGGGTTTG
ALK12ex-R	ATCTCCCCATCTCCAACCTT
ALK13ex-F	GAAGTGGGGGAGAAGAATCC
ALK13ex-R	AACTTCCAGGAGGAGGGTGT
ALK14ex-F	TTCTGTCTGCTGCAAAGTGG
ALK14ex-R	TCATGAGGCTCTGACATTGC
ALK15ex-F	GAAGCACAGCTCGGTTTCTC
ALK15ex-R	AGCTCCAGGTCAGCAAGATG
ALK16ex-F	GCCAGCATGGCTAATTGAAC
ALK16ex-R	GGACTAAGCAGGGAGGGAGT
ALK17ex-F	CCCAGTGACCCCCTAACTTT
ALK17ex-R	TTAGCTTGGTGGGAGGACTG
ALK18ex-F	TCCAGTGGCTATGGGACCTA
ALK18ex-R	CATGACCCACCTTTCACACA
ALK19ex-F	CTCATGGTCCCCTGAAAAGA
ALK19ex-R	TCACCATCGTGATGGACACT
ALK20ex-F	TCAGAGCTCAGGGGAGGATA
ALK20ex-R	GAGTCTGCGGTGCTGTGATA
ALK22_21ex-F	CCCAGCTGCCTCATTATTGT
ALK22_21ex-R	AACCATCAAGGGTTGTTCCA
ALK23ex-F	ACCTGCTCACCAGCAAGATT
ALK23ex-R	TCCATTCTCTTCCACCCAGT
ALK24ex-F	CATTTCCCCTAATCCTTTTCCA
ALK24ex-R	GTGATCCCAGATTTAGGCCTTC
ALK25ex-F	GCCTCTCGTGGTTTGTTTTGTC
ALK25ex-R	CCCAGGGTAGGGTCCAATAATC
ALK26ex-F	CCTGCTCTCCTCCTGAACC
ALK26ex-R	CAGGGATACCTGGAGGATGA
ALK27ex-F	GAATGTGGGTGGGTGTGTCT
ALK27ex-R	CAGTCACATTCGCATCTTGG
ALK28ex-F	CCTTTACACCTGCGCACTCT
ALK28ex-R	AAATGGGCAAATGGAGACAC
ALK29-1F	AAATCCTGGTTTCCTCATCTG
ALK29-1R	GTGTGGCTCCTTCTTTGCTA
ALK29-2F	AAGGGGGACACGTGAATATG
ALK29-2R	TTGGCACAAAACAAAACGTG

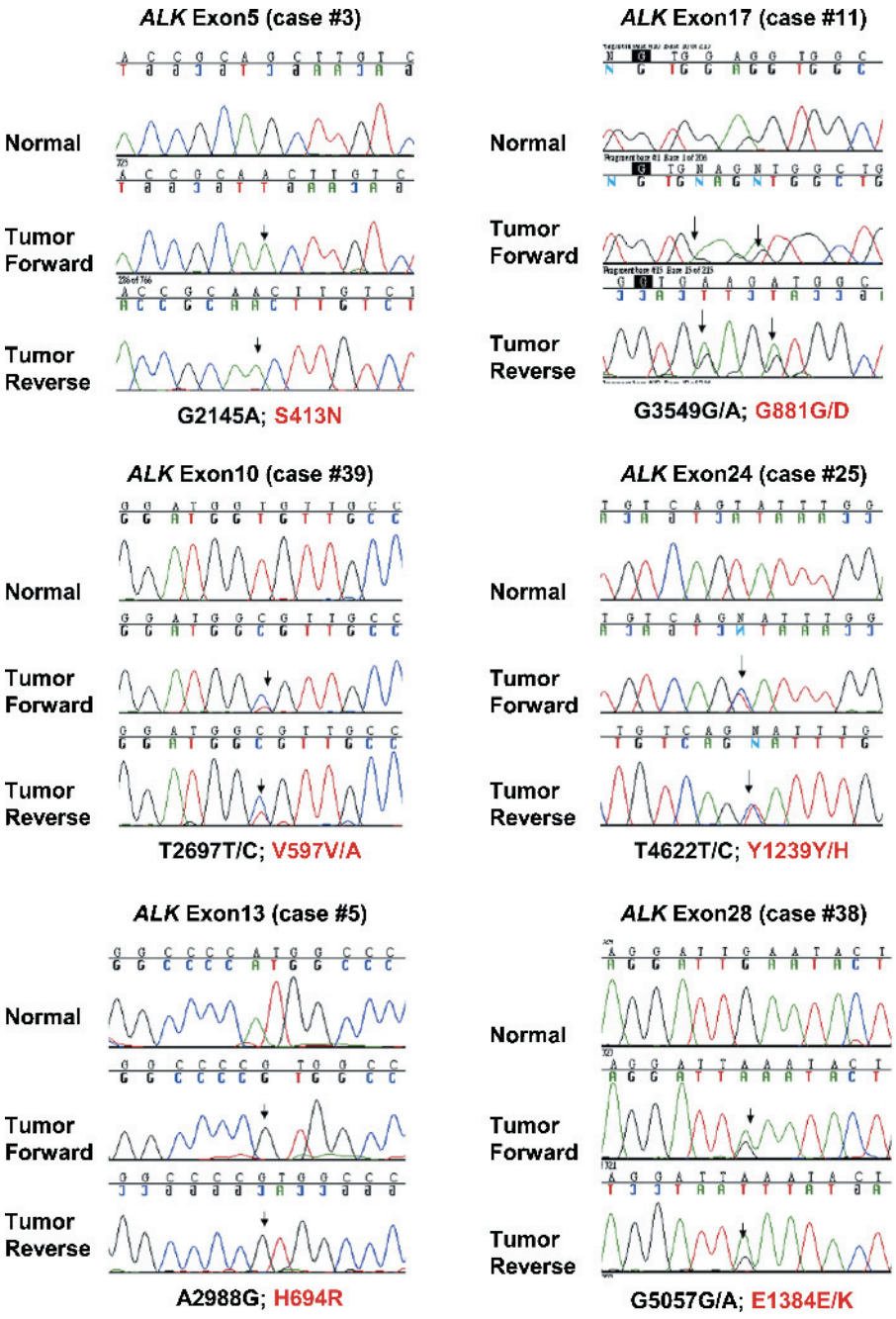

Figure W1. Electropherograms of six ALK somatic mutations. Snapshots of mutations are presented after alignment of sequencing data from the paired tumor and tumor-adjacent normal tissues of lung adenocarcinoma with majority of the forward and reversed sequencing validation.

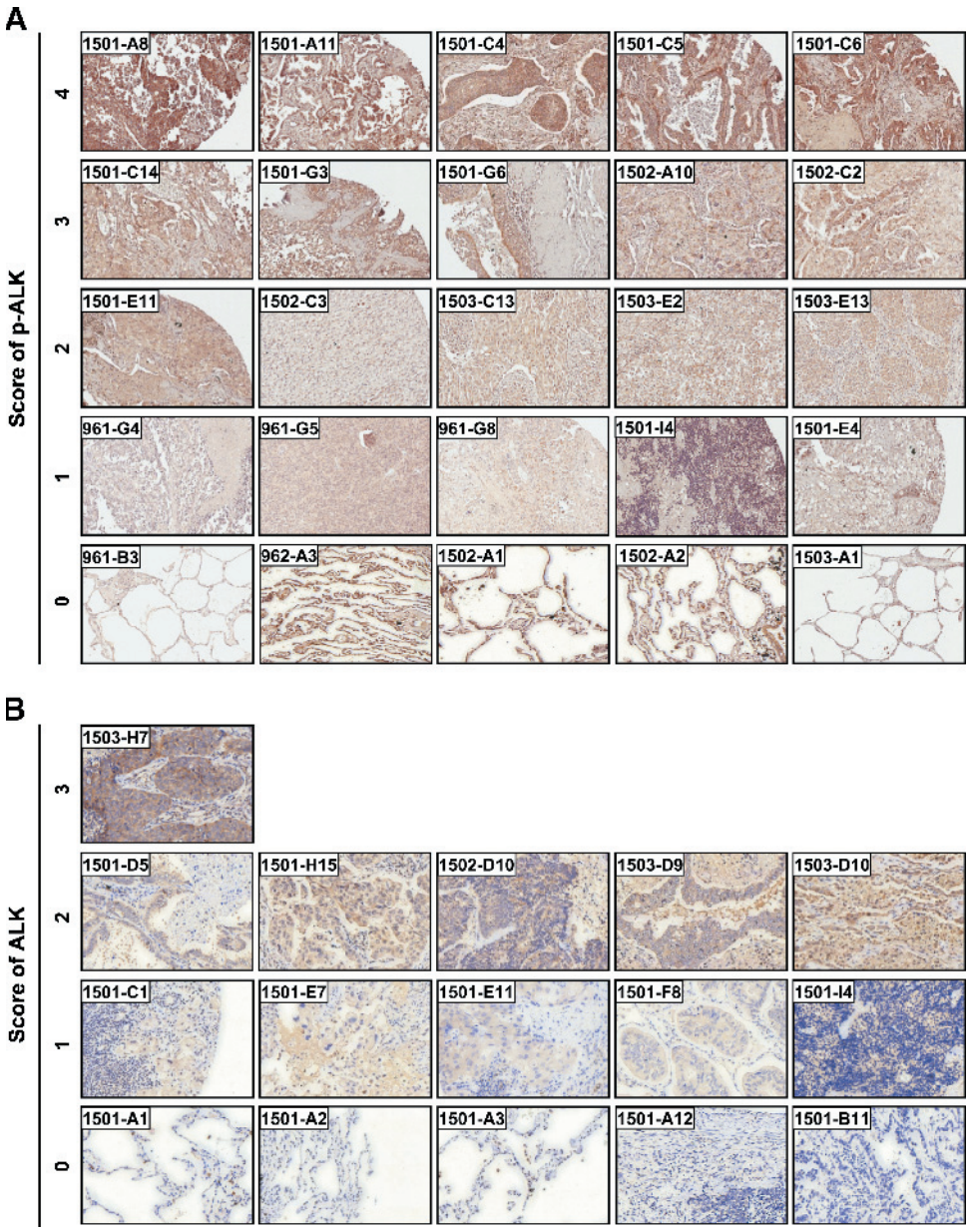

Figure W2. Representative images of IHC scoring intensity of phosphorylated Y1604 (A) and total ALK (B) in sections of lung cancer patients ranked from 0 to 4 randomly selected from the indicated tissue arrays.

Table W3. Correlation between Phosphorylated Y1064 ALK and Total ALK Expression.

IHC Staining Antibody	*n*	IHC Intensity	*P*
Phospho-ALK	263	2.9684 ± 0.6852	
ALK	263	1.2274 ± 0.7707	.4449

Data show mean ± SD.
No correlation between p-ALK and ALK (Pearson coefficient, r = 0.04703).

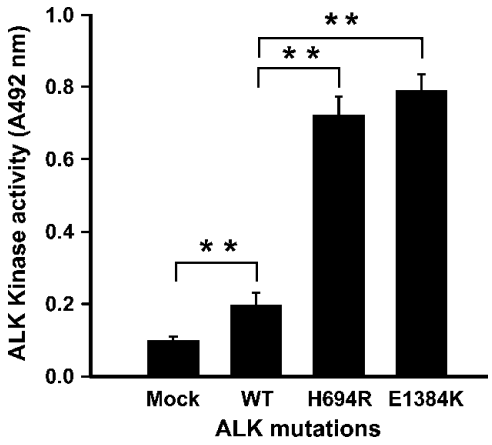

Figure W3. *In vitro* kinase activity of ALK mutations H694R and E1384K. The ALK activities of wild-type, H694R, and E1384K ALK mutations in H1299 stable cells were measured by ELISA reactions at 492 nm. Data are shown as mean ± SD. $^{**}P < .001$.

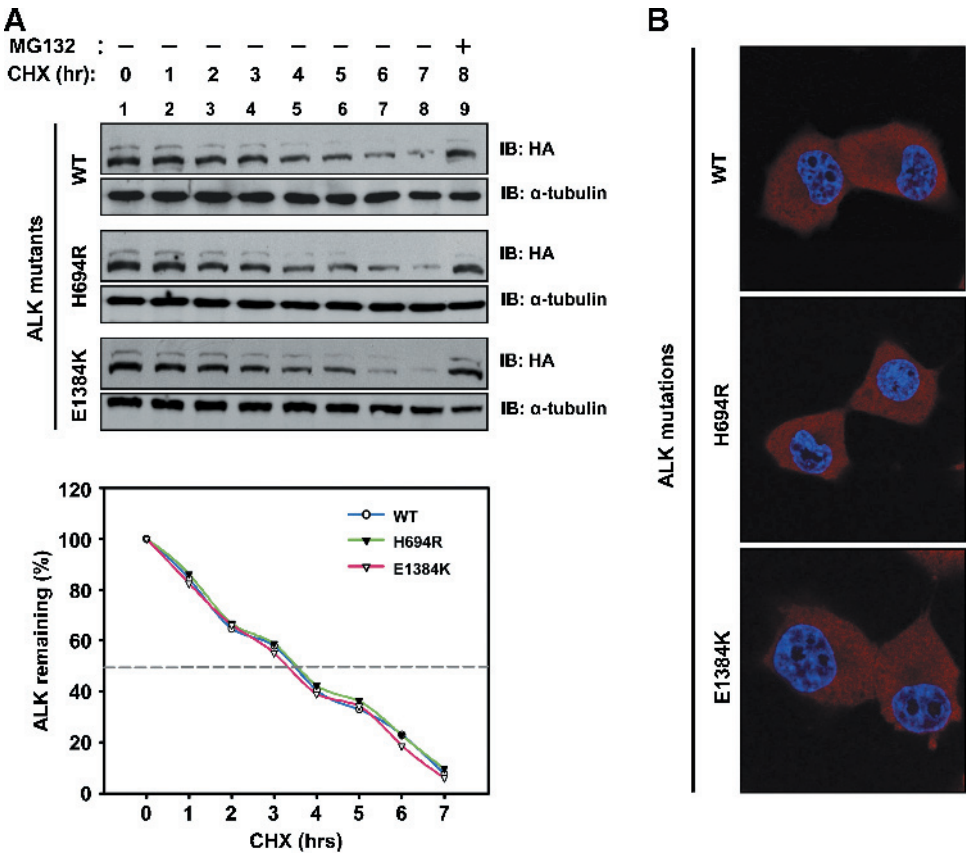

Figure W4. Protein stability and subcellular localization of H694R and E1384K. (A) Protein stability of H694R and E1384K. The ALK protein expression of H1299 cells that stably expressed wild-type, H694R, and E1384K ALK mutations was examined after cycloheximide treatment by Western blot analysis using anti-HA antibody (top panel). Addition of MG132 to stop protein degradation is used as a positive control. The remaining protein quantification is shown at the bottom panel, and the half-life of ALK protein is labeled with a dashed line. (B) Subcellular localization of H694R and E1384K. The immunofluorescence image for ALK protein was examined in H1299 cells that stably expressed wild-type, H694R, and E1384K ALK mutations.

Table W4. IC_{50} of WHI-P154 in ALK Mutations.

ALK	IC_{50} (Cell Proliferation Inhibition by WHI-P154; μM)
WT	26.9375
H694R	11.7901
E1384K	9.4238

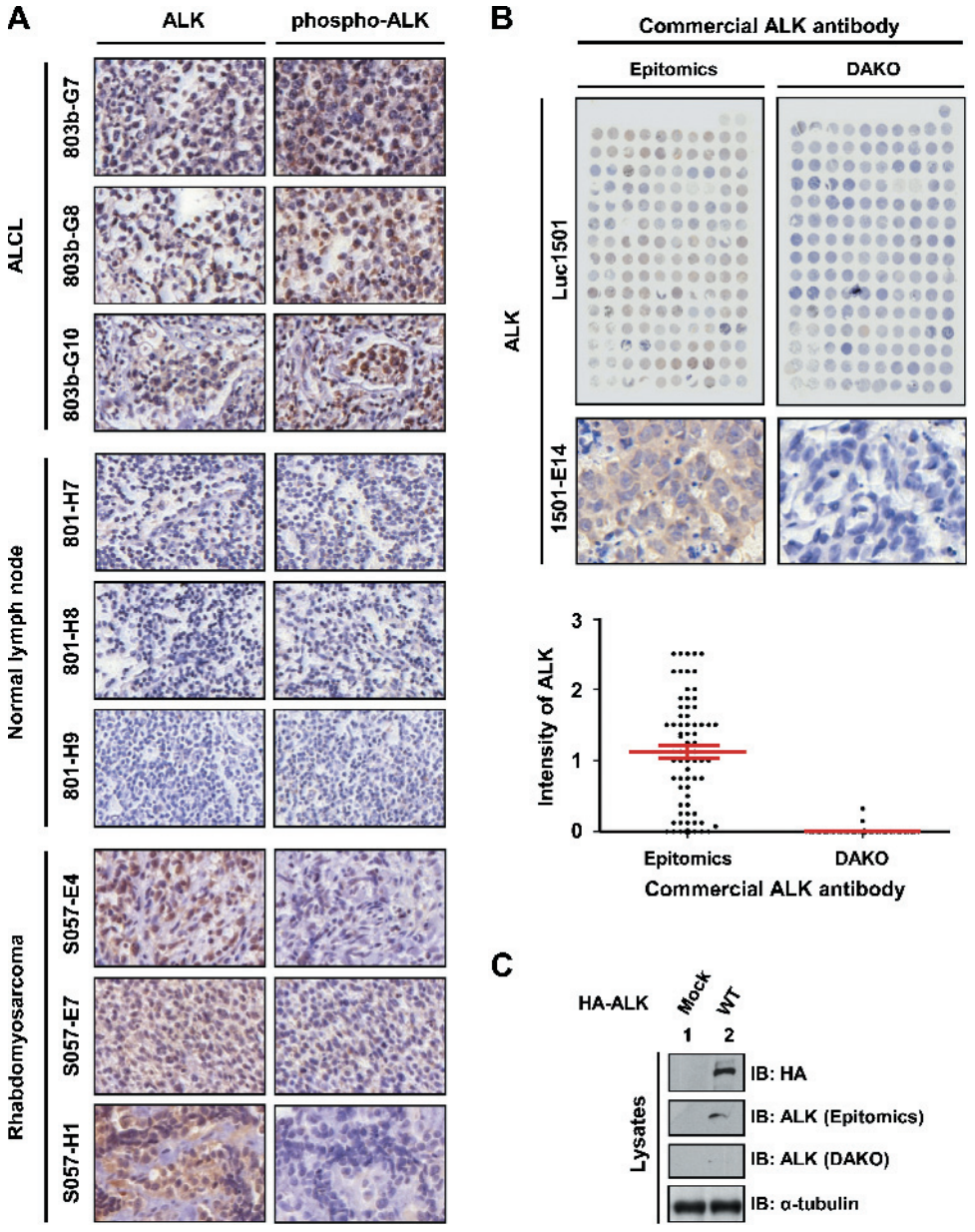

Figure W5. Comparisons of phospho-Y1604 and total ALK antibodies using IHC and Western blot analyses. (A) IHC analysis on sections of ALCL, rhabdomyosarcoma, and normal lymph node with phospho-Y1604 ALK antibody (right panel) and total ALK antibody (left panel) from Epitomics. (B) Lung cancer tissue arrays (Biomax) from the same patients were used to compare the expression intensity of ALK protein by IHC assay using two ALK antibodies. The IHC results of the entire arrays (Luc1501) and a representative image (1501-E14) are shown at the upper panel, and the quantification result is shown at the bottom panel. (C) Lysates of H1299 cells that stably expressed wild-type ALK were used to examine the sensitivity of these two ALK antibodies by Western blot analysis. Anti-HA antibody served as a positive control for HA-ALK expression, and the α-tubulin served as a loading control.

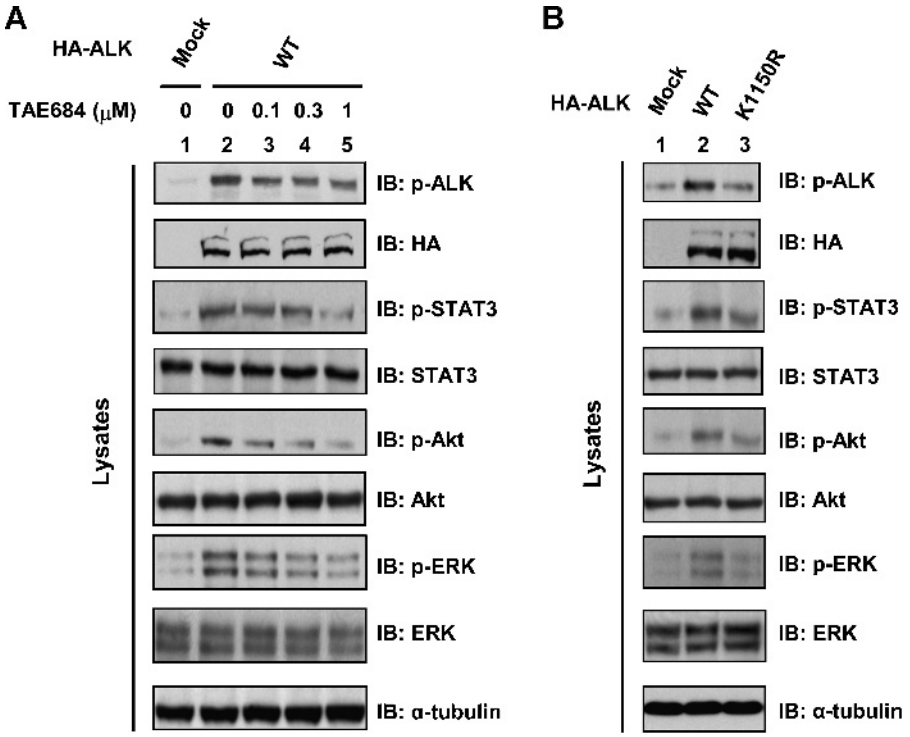

Figure W6. Overexpression of wild-type ALK enhanced p-STAT3, p-AKT, and p-ERK protein expression in a kinase-dependent manner. (A) Treatment of TAE684 on wild-type ALK overexpressing H1299 cells decreased p-STAT3, p-AKT, and p-ERK expression in a dose-dependent manner detected by Western blot analysis. (B) Overexpression of ALK K1150R kinase-dead mutant and mock control in H1299 has no effects on the phosphorylation of the protein expression levels of p-Y1604 ALK, p-STAT3, p-AKT, and p-ERK by Western blot analysis. The α-tubulin served as a loading control.

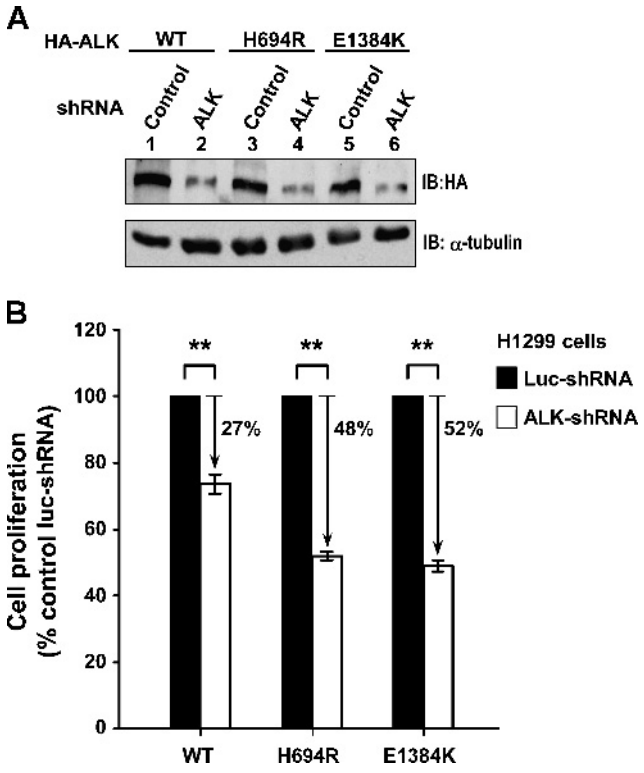

Figure W7. ALK down-regulation (A) and growth-inhibitory effects (B) of ALK shRNA treatments on wild-type, mutant H694R, and E1384K ALK transfectants of H1299 cells. The luciferase shRNA was the control. The α-tubulin served as a loading control.